

# Histological Predictors of Maximum Failure Loads Differ Between the Healing ACL and ACL Grafts After 6 and 12 Months In Vivo

Benedikt L. Proffen,<sup>\*†</sup> MD, Braden C. Fleming,<sup>‡</sup> PhD, and Martha M. Murray,<sup>†</sup> MD

*Investigation performed at Boston Children's Hospital, Department of Orthopaedic Surgery and Sports Medicine, Harvard School of Medicine, Boston, Massachusetts, USA*

**Background:** Bioenhanced anterior cruciate ligament (ACL) repair, where the suture repair is supplemented with a biological scaffold, is a promising novel technique to stimulate healing after ACL rupture. However, the histological properties of a successfully healing ACL and how they relate to the mechanical properties have not been fully described.

**Purpose:** To determine which histological features best correlate with the mechanical properties of the healing ACL repairs and ACL grafts in a porcine model at 6 and 12 months after injury.

**Study Design:** Controlled laboratory study.

**Methods:** A total of 48 Yucatan mini-pigs underwent ACL transection followed by: (1) conventional ACL reconstruction with bone–patellar tendon–bone (BPTB) allograft, (2) bioenhanced ACL reconstruction with BPTB allograft using a bioactive scaffold, or (3) bioenhanced ACL repair using the same bioactive scaffold. After 6 and 12 months of healing, structural properties of the ACL or graft (yield and failure load, linear stiffness) were measured. Following mechanical testing, ACL specimens were histologically analyzed for cell and vascular density and qualitatively assessed using the advanced Ligament Maturity Index.

**Results:** After 6 months of healing, the cellular organization subscore was most predictive of yield load ( $r^2 = 0.98$ ), maximum load ( $r^2 = 0.89$ ), and linear stiffness ( $r^2 = 0.95$ ) of the healing ACL, while at 12 months, the collagen subscore ( $r^2 = 0.68$ ) became the best predictor of maximum load. For ACL grafts, the reverse was true, with the collagen subscore predictive of yield and maximum loads at 6 months ( $r^2 = 0.55$ ) and graft cellularity predictive of maximum load of the graft at 12 months ( $r^2 = 0.50$ ).

**Conclusion:** These findings suggest there may be key biological differences in development and maintenance of ACL tissue after repair or reconstruction, with early ligament function dependent on cellular population of the repair but early graft function dependent on the maintenance of organized collagen.

**Clinical Relevance:** Bioenhanced ACL repair shows promising potential as an alternative clinical treatment for ACL injury. This study contributes to the understanding of the cellular contribution to mechanical characteristics of the healing ACL in both repaired and reconstructed ACLs.

**Keywords:** bioenhanced ACL repair; ACL reconstruction; Ligament Maturity Index; biomechanical properties

\*Address correspondence to Benedikt L. Proffen, MD, Boston Children's Hospital, Department of Orthopaedic Surgery and Sports Medicine, Harvard School of Medicine, 300 Longwood Avenue, Boston, MA 02115, USA (e-mail: benedikt.proffen@childrens.harvard.edu).

†Boston Children's Hospital, Department of Orthopaedic Surgery, Harvard School of Medicine, Boston, Massachusetts, USA.

‡Rhode Island Hospital, Department of Orthopaedics, Warren Alpert Medical School, Brown University, Providence, Rhode Island, USA.

The contents of this article are solely the responsibility of the authors and do not necessarily represent the official views of the National Institutes of Health or the National Institute of Arthritis and Musculoskeletal and Skin Diseases (NIAMS).

One or more of the authors has declared the following potential conflict of interest or source of funding: M.M.M. and B.C.F. have patents and/or patents pending related to the material presented in this article. This investigation was supported by National Institutes of Health under NIAMS (1RO1-AR056834, 1RO1-AR056834S1 [ARRA], and 2RO1-AR054099), as well as the Lucy Lippitt Endowment.

The Orthopaedic Journal of Sports Medicine, 1(6), 2325967113512457  
DOI: 10.1177/2325967113512457

© The Author(s) 2013

Approaches to enhance the healing of anterior cruciate ligament (ACL) tissue and ACL grafts using tissue engineering techniques have recently become of interest.<sup>7,9,12,14</sup> Bioenhanced ACL repair is a new technology where an extracellular matrix scaffold is placed between the torn ligament ends to stimulate fibrovascular scar formation.<sup>20</sup> For bioenhanced ACL reconstruction, a similar scaffold is placed around an ACL graft in an effort to enhance healing and improve the strength of the graft.<sup>9</sup> The histological qualities of the fibrovascular scar tissue or the graft in relation to its biomechanical properties over time are as yet unknown. While biomechanical testing provides an indicator of healing following surgery, it does not provide an explanation as to how this improvement in strength or stiffness is achieved and what factors contribute to the improvement on a cellular or tissue level. As we enter into the biological era of sports medicine surgery, knowledge of how the repaired or reconstructed ligament is histologically organized and how that organization evolves over time

postoperatively may provide insight as to the future, longer term performance of the healing or reconstructed ACL.

The Ligament Maturity Index (LMI) has previously been proposed to score the histological preparations of the early stages of healing ligaments.<sup>18</sup> The LMI was first published in 2007 in a study on canine ligament healing<sup>18</sup> and was based on prior reports of histological features of successfully healing connective tissues, including ligaments and tendons. The LMI has 3 subscores—cell, collagen, and vessel—which are then summed to make a total score. Although the LMI provides a valid means to describe the histological appearance of healing ligaments, the initial LMI was focused on the early inflammatory and proliferative phases of ligament healing. Although used to document ligament healing, the LMI has not been previously applied to quantify ACL graft healing after reconstruction, where the process of “ligamentization” involves repopulation of the graft with cells and a gradual reorganization of the tendinous tissue that more closely resembles ligament tissue (with a shorter crimp formation).<sup>3</sup> The relationship between histological features and the later stages of ligament healing and graft incorporation have not yet been defined.

We recently conducted a long-term (6- and 12-month) study of bioenhanced ACL repair and ACL reconstruction.<sup>16</sup> The early version of the LMI had multiple criteria that were less applicable to the later stages of the proliferative and remodeling phases. For these reasons, prior to scoring the specimens for this longer term study, we recently modified it for use in the later stages of healing to create the “advanced LMI.” For example, the cellular subscore for the LMI had a maximum score of 2 points for a “less than 2× normal” number of fibroblasts. To reflect the later time points where the tissues would be expected to have a fibroblast number closer to “normal,” the criteria of “less than 1.5× normal” was added, and the “no cell” category was scored with –1 points. Similar changes were made for the cellularity and collagen scores (Table 1), with additional categories added for improvements in cellularity, collagen organization, and vascularity.

In this study, we hypothesized that the histological quality of healing ACL tissue following bioenhanced ACL repair at 6 and 12 months of healing, as measured by the advanced LMI and its subscores, would be predictive of the structural properties (eg, yield and failure loads and linear stiffness) and material properties (stress, strain, tangent modulus) of the healing tissue at both time points. In addition, we hypothesized that the histological quality of the reconstructed ACL would also be predictive of the structural and material properties of the graft. To evaluate the hypotheses, we used the established mini-pig model of ACL healing and reconstruction.<sup>16</sup>

## MATERIALS AND METHODS

### Study Design

Institutional Animal Care and Use Committee approvals were obtained prior to initiating the study. Forty-eight Yucatan mini-pigs with closed tibial and femoral physes (mean age ±

TABLE 1  
Criteria Used to Generate the Advanced Ligament Maturity Index for Healing Ligaments and Graft Tissue

Advanced Ligament Maturity Index	Points (Total = 26 Points)
<b>Cellularity subscore (total = 8 points)</b>	
Presence of inflammatory cells	
Necrosis	0
Polymorphonuclear cells	1
No inflammatory cells	2
Number of fibroblasts	
None	–1
>2× normal	0
1.5× to 2× normal	1
<1.5× normal	2
Nuclear aspect ratio (NAR) of fibroblasts	
No cells	–1
Average NAR <2 (round)	0
Average NAR 2-4	1
Average NAR >4 (elongated)	2
Orientation: Long axis of nucleus parallel with normal fascicles	
No cells	–2
<30% of cells oriented to long axis of ligament	–1
30%-50% oriented	0
50%-75% oriented	1
75%-100% oriented	2
<b>Collagen subscore (total = 12 points)</b>	
Width of bundles	
No bundles	0
Width <50 μm	2
Width >50 μm	4
Bundle orientation	
No bundles	–2
<50% oriented to long axis of ligament	0
50%-75% oriented	2
75%-100% oriented	4
Crimp	
No crimp	–2
<25% crimp	0
25%-75% crimp	2
Crimp with normal length present	4
<b>Vascularity subscore (total = 6 points)</b>	
Density of blood vessels	
None present	–1
>200% present	0
150%-200% present	1
<150% present	2
Orientation of vessels with long axis of ligament	
No vessels oriented	–2
<30% oriented	–1
<50% oriented	0
50%-75% oriented	1
75%-100% oriented	2
Vessel maturity	
No vessels seen	0
Capillaries only present	1
Arterioles present	2

standard deviation [SD], 15.0 ± 0.95 months; weight, 58.6 ± 7.9 kg) underwent unilateral ACL transection and were then randomized to 1 of 3 experimental groups (Figure 1):

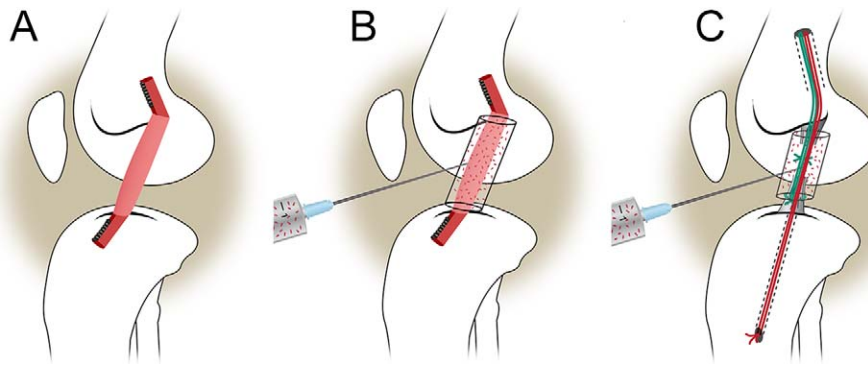


**Figure 1.** Schematic of the 3 treatment groups: (A) traditional ACL reconstruction, (B) bioenhanced ACL reconstruction using the ECM scaffold soaked in blood, and (C) bioenhanced ACL repair using the ECM scaffold soaked with blood. ACL, anterior cruciate ligament; ECM, extracellular matrix. (Adapted from Murray MM, Fleming BC. Use of a bioactive scaffold to stimulate anterior cruciate ligament healing also minimizes post-traumatic osteoarthritis after surgery. *Am J Sports Med.* 2013;41:1762-1770; reprinted with permission.)

(1) conventional ACL reconstruction with bone–patellar tendon–bone (BPTB) allograft,<sup>20</sup> (2) bioenhanced ACL reconstruction with BPTB allograft using a bioactive scaffold,<sup>9</sup> and (3) bioenhanced ACL repair using the same bioactive scaffold.<sup>17</sup> Half of the animals within each treatment group were allowed to heal for 6 and 12 months, respectively.

#### Preparation of the Extracellular Matrix Scaffold

The bioactive scaffolds (MIACH; Boston Children’s Hospital, Boston, Massachusetts, USA) were manufactured as previously described.<sup>17</sup> A slurry of extracellular matrix proteins was produced from bovine tissue. The slurry was lyophilized in a mold to produce the desired shape. For the bioenhanced ACL reconstruction group, the scaffold was formed into a porous hollow cylinder with an outer diameter of 22 mm, inner diameter of 10 mm, and length of 30 mm.<sup>17</sup> For the bioenhanced ACL repair group, the scaffolds were formed into a porous cylinder 22 mm in diameter and 30 mm in length.<sup>9</sup> When implanted in the joint, the scaffolds were activated with the addition of autologous blood.

#### ACL Reconstruction and Bioenhanced ACL Reconstruction

A medial arthrotomy was created and the fat pad partially resected to expose the ACL. The ACL was cut between the proximal and middle thirds of the ligament with a scalpel. A Lachman test was performed to verify complete ACL transection. ACL reconstruction using fresh-frozen BPTB allografts was performed as previously described.<sup>9</sup> The entire patellar tendon (approximately 10 mm in width) was used for the soft tissue portion of the graft. The grafts were firmly tensioned with the knee in maximal extension (30°), and the distal block was secured in the tibia using a second 6-mm interference screw (Biosure; Smith & Nephew, Andover, Massachusetts, USA).

For the animals in the bioenhanced ACL reconstruction group, the same ACL reconstruction procedure was performed; however, after femoral graft fixation, the cylindrical extracellular matrix–based scaffold was threaded over

the graft and positioned to cover the intra-articular portion. The distal bone plug was then seated retrograde into the tibial tunnel and fixed to the tibia using a second 6-mm interference screw. Three milliliters of autologous blood were used to saturate the scaffold in situ.

#### Bioenhanced ACL Repair

After ACL transection was performed, a bioenhanced ACL repair was performed as previously described.<sup>17</sup> In brief, a button carrying 3 looped sutures was secured on the femur proximally. The scaffold was threaded onto 2 of the sutures and slid up into the notch adjacent to the femoral ACL stump. The ends of the sutures were then passed into a pre-drilled tibial tunnel and fixed extracortically using a second button with the knee in maximum extension (30°). The remaining suture was tied to a Kessler suture of No. 1 Vicryl (Ethicon, Somerville, New Jersey, USA), which had been placed in the tibial stump of the ACL (Figure 1).<sup>8</sup> Three milliliters of autologous blood were used to saturate the scaffold in situ.

Following surgery, all animals were housed for 4 weeks in individualized pens and were then shipped to a farm for long-term porcine care (Coyote Consulting Corp Inc, Douglas, Massachusetts, USA). After 6 and 12 months of healing, the animals were euthanized, the limbs harvested, and the knees frozen at –20°C until mechanical testing.

#### Biomechanical Testing

The knees were prepared for biomechanical testing as previously described.<sup>9</sup> The biomechanical testing procedures (ie, structural properties) were performed using a servohydraulic load frame and custom fixtures (MTS Systems Corp, Eden Prairie, Minnesota, USA).<sup>9</sup> All investigators were blinded to the treatment group during specimen preparation and testing. The structural properties of the ligaments and grafts were determined using a standardized failure test protocol.<sup>12</sup> Before starting the tensile test, the femur was lowered until the load across the joint surface was +5 N of compression. A ramp at 20 mm/min was initiated, and the

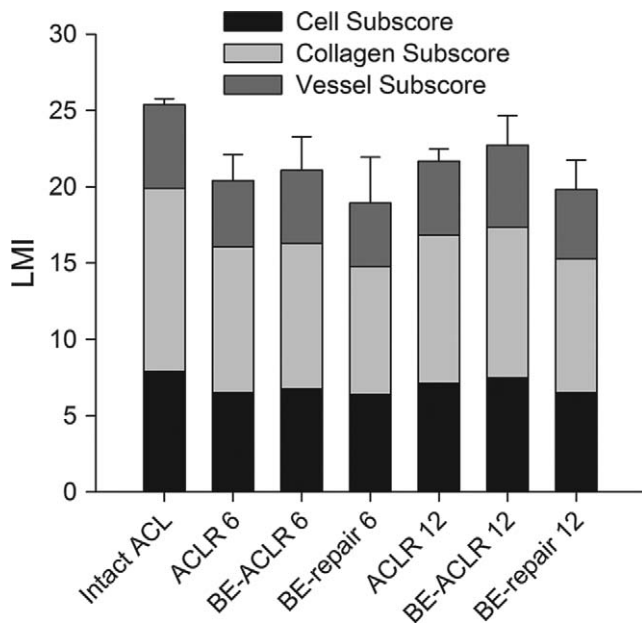


**Figure 2.** Bar graph of the mean values of the advanced Ligament Maturity Index (LMI) score of the different treatment groups at 6 and 12 months. Individual bars show the contribution of the subscores (cellularity, collagen, vascularity) to the total score. Error bars show the 95% confidence intervals of the means. ACLR 6, anterior cruciate ligament (ACL) reconstruction after 6 months; ACLR 12, ACL reconstruction after 12 months; BE, bioenhanced.

load-displacement data were recorded at 100 Hz.<sup>13</sup> The yield load, failure load, and linear stiffness were determined from the MTS load-displacement data. These biomechanical data were previously reported.<sup>16</sup> Material properties of the ligaments (stress, strain, and tangent modulus) were also calculated from the load displacement tracing of the failure test using the cross-sectional area and initial length of the ACL to calculate the stress and strain, respectively, both of which were measured before biomechanical testing using a caliper. To calculate the cross-sectional area, an elliptical cross section was assumed.

**Histology**

After mechanical testing, the knees were cut along the sagittal plane through the ACL tissue (repaired ligament or graft). All tissues were then fixed in formalin and decalcified (DELTA-Cal; Delta Products Group, Aurora, Illinois, USA). The knee sections were then dehydrated, embedded in paraffin, and microtomed into 7-µm sections. These sections were placed onto custom glass slides (Corning 75 × 50-mm Plain Microscope Slides; Corning Inc, Corning, New York, USA) and stored at 4°C until staining with hematoxylin and eosin or α-smooth muscle actin antibodies.<sup>12</sup> Hematoxylin and eosin staining was used to determine cell density and collagen formation, which was scored using polarized light with a wavelength filter at 137 nm, while α-smooth

**TABLE 2**  
Mechanical Properties of the Healing Ligament/Graft Versus Histological Parameters<sup>a</sup>

Group	Yield Load		Maximum Load		Linear Stiffness	
	r <sup>2</sup>	P	r <sup>2</sup>	P	r <sup>2</sup>	P
<b>Bioenhanced repair</b>						
6 months (n = 8)						
LMI	0.75 <sup>b</sup>	<.01	0.76 <sup>b</sup>	<.01	0.79 <sup>b</sup>	<.01
Cell subscore	0.98 <sup>b</sup>	<.001	0.89 <sup>b</sup>	<.001	0.95 <sup>b</sup>	<.001
Collagen subscore	0.60 <sup>b</sup>	<.05	0.67 <sup>b</sup>	<.05	0.66 <sup>b</sup>	<.05
Vessel subscore	0.38	.1	0.33	.14	0.44	.07
Cell density	0.06	.57	0.01	.92	0.04	.62
Vessel density	0.01	.97	0.02	.76	0.01	.96
12 months (n = 8)						
LMI	0.28	.18	0.51 <sup>b</sup>	<.05	0.45	.08
Cell subscore	0.01	.85	0.17	.31	0.1	.45
Collagen subscore	0.58 <sup>b</sup>	<.05	0.68 <sup>b</sup>	<.05	0.53 <sup>b</sup>	<.05
Vessel subscore	0.05	.6	0.07	.54	0.2	.27
Cell density	0.03	.69	0.25	.21	0.14	.36
Vessel density	0.03	.7	0.04	.64	0.15	.35
<b>ACL reconstruction</b>						
6 months (n = 8)						
LMI	0.89 <sup>b</sup>	<.001	0.83 <sup>b</sup>	<.01	0.59 <sup>b</sup>	<.05
Cell subscore	0.15	.34	0.11	.42	0.11	.43
Collagen subscore	0.62 <sup>b</sup>	<.05	0.55 <sup>b</sup>	<.05	0.27	.19
Vessel subscore	0.54 <sup>b</sup>	<.05	0.62 <sup>b</sup>	<.05	0.70 <sup>b</sup>	<.01
Cell density	0.02	.76	0.01	.79	0.00	.99
Vessel density	0.04	.64	0.05	.6	0.02	.75
12 months (n = 8)						
LMI	0.12	.41	0.02	.73	0.01	.82
Cell subscore	0.12	.39	0.04	.64	0.31	.15
Collagen subscore	0.44	.07	0.24	.21	0.01	.80
Vessel subscore	0.02	.74	0.01	.93	0.17	.32
Cell density	0.24	.22	0.73 <sup>b</sup>	<.01	0.54 <sup>b</sup>	<.05
Vessel density	0.13	.38	0.17	.32	0.01	.98
<b>Bioenhanced ACL reconstruction</b>						
6 months (n = 8)						
LMI	0.34	.13	0.52 <sup>b</sup>	<.05	0.11	.42
Cell subscore	0.06	.54	0.11	.42	0.05	.61
Collagen subscore	0.21	.25	0.45	.07	0.23	.23
Vessel subscore	0.21	.26	0.16	.33	0.01	.95
Cell density	0.29	.16	0.17	.31	0.11	.42
Vessel density	0.32	.14	0.06	.56	0.07	.54
12 months (n = 8)						
LMI	0.01	.99	0.01	.93	0.06	.57
Cell subscore	0.09	.48	0.17	.31	0.11	.44
Collagen subscore	0.01	.96	0.01	.93	0.02	.73
Vessel subscore	0.02	.78	0.03	.66	0.13	.39
Cell density	0.24	.22	0.22	.24	0.24	.21
Vessel density	0.03	.7	0.09	.48	0.16	.33

<sup>a</sup>Shown are linear regression coefficients and P values at 6 and 12 months for each of the 3 groups. LMI, Ligament Maturity Index; ACL, anterior cruciate ligament.

<sup>b</sup>Statistically significant correlation.

muscle actin immunohistochemistry was used to determine vascularity. Quantitative analysis of the cell density and vascular density were performed by an observer who was blinded to the treatment groups and time points of the photomicrographs.

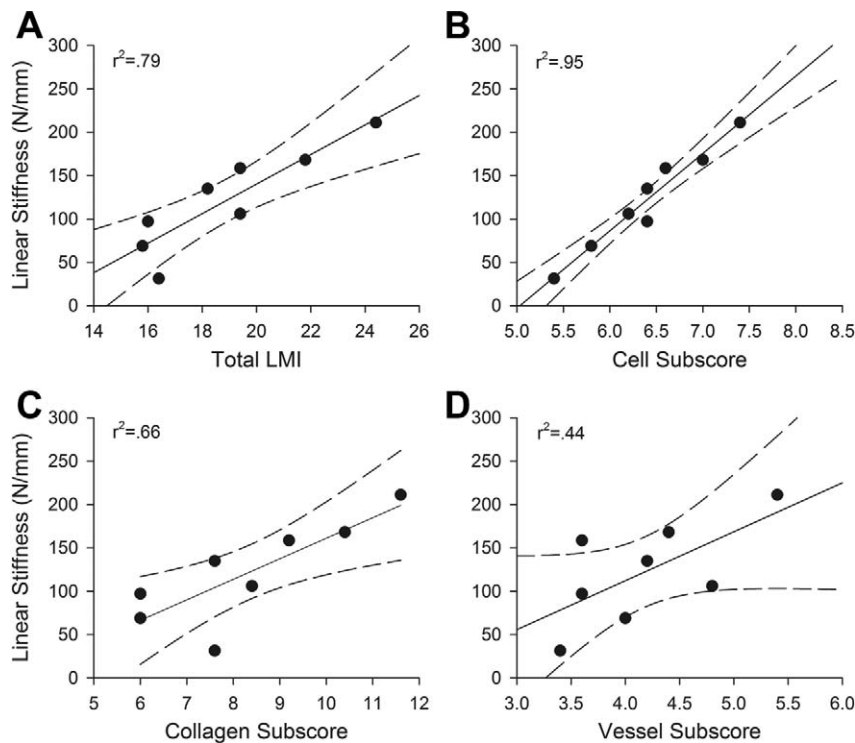


**Figure 3.** Linear stiffness of the bioenhanced ACL repair procedure at 6 months of healing as a function of (A) total LMI, (B) cellular subscore, (C) collagen subscore, and (D) vessel subscore. Dotted lines are 95% confidence intervals for slope. A higher LMI in the repair tissue correlated with higher linear stiffness of the tissue, with the cellular subscore resulting in the strongest correlation. Maximum load had similar correlations. ACL, anterior cruciate ligament; LMI, Ligament Maturity Index.

### Histological Scoring

The advanced LMI (Table 1) was used to assess the ACL tissue (repair tissue or graft). Sagittal sections through the middle of each healing ligament or graft were analyzed. Analysis was performed for 5 regions of the ligament, each region measuring 1 mm in length and spanning the entire width of the ligament tissue. The synovium was excluded from the analysis. The 5 regions that were analyzed were as follows: 1 mm from the femoral insertion site, 1 mm from the tibial insertion site, and 3 regions in between those 2 regions, with the exclusion of the zone deformed by the biomechanical testing.<sup>12</sup> In addition to the advanced LMI scoring performed for the larger regions, the total number of cells and vessels in each of the 5 regions were counted in a discrete central area of 0.08 mm<sup>2</sup> and 1.4 mm<sup>2</sup>, respectively.<sup>12</sup>

### Statistical Methods

The data collected from the histological and biomechanical analyses were analyzed using the Kolmogorov-Smirnov test, which verified the normal Gaussian distribution of the data sets. Then, applying the linear regression model between the histological scores and the biomechanical data, we analyzed predictability of the biomechanical properties by the histological parameters. The advanced LMI of the wound site and its subscores

(cell, vessel, collagen) as well as the cell and vessel densities were the independent variables. We tested the bivariate association of these endpoints with the dependent variables representing the biomechanical structural properties (yield load, maximum failure load, and linear stiffness) and material properties (yield stress, maximum failure stress, tangent modulus). Independent regressions were performed for the 6- and 12-month specimens. Differences in the dependent variables between the groups were assessed using a 1-way analysis of variance. Bonferroni correction was utilized for multiple comparisons. All analyses were performed using Intercooled STATA 11 (Stata Corp LP, College Station, Texas, USA). An  $\alpha$  value of 5% was considered significant. All data are presented as means with 95% confidence intervals.

## RESULTS

### Bioenhanced Repairs: 6 months

For the bioenhanced repairs, the total advanced LMI (Figure 2) predicted 76% of the variability of the structural properties (maximum load and linear stiffness) of the healing tissue after 6 months of healing ( $r^2 > 0.76$ ,  $P < .01$  for both comparisons) (Table 2, Figure 3). The cellular subscore was also significantly predictive of the structural properties (maximum load and stiffness) of the healing tissue ( $r^2 > 0.89$ ,  $P < .001$  for both

TABLE 3  
Material Properties of the Healing Ligament/Graft Versus Histological Parameters<sup>a</sup>

Group	Yield Stress		Maximum Stress		Yield Strain		Maximum Strain		Tangent Modulus	
	$r^2$	$P$	$r^2$	$P$	$r^2$	$P$	$r^2$	$P$	$r^2$	$P$
<b>Bioenhanced repair</b>										
6 months (n = 8)										
LMI	0.07	.52	0.08	.50	0.00	.93	0.00	.92	0.07	.54
Cell subscore	0.07	.52	0.07	.54	0.01	.82	0.00	.92	0.06	.55
Collagen subscore	0.13	.38	0.15	.35	0.00	.99	0.01	.84	0.12	.4
Vessel subscore	0.05	.61	0.04	.62	0.00	.93	0.01	.86	0.06	.56
Cell density	0.06	.56	0.01	.92	0.15	.34	0.42	.08	0.04	.64
Vessel density	0.06	.57	0.04	.66	0.01	.80	0.15	.34	0.08	.49
12 months (n = 8)										
LMI	0.75 <sup>b</sup>	<.01	0.71 <sup>b</sup>	<.01	0.05	.63	0.04	.65	0.44	.07
Cell subscore	0.72 <sup>b</sup>	<.01	0.56 <sup>b</sup>	<.05	0.17	.31	0.02	.72	0.06	.57
Collagen subscore	0.52 <sup>b</sup>	<.05	0.59 <sup>b</sup>	<.05	0.02	.75	0.15	.34	0.3	.16
Vessel subscore	0.12	.39	0.19	.28	0.11	.43	0.29	.17	0.35	.12
Cell density	0.02	.70	0.00	.97	0.09	.47	0.01	.83	0.01	.86
Vessel density	0.00	.96	0.00	.92	0.17	.31	0.31	.15	0.01	.75
<b>ACL reconstruction</b>										
6 months (n = 8)										
LMI	0.06	.57	0.13	.38	0.31	.15	0.21	.26	0.03	.69
Cell subscore	0.37	.11	0.13	.38	0.4	.09	0.04	.65	0.03	.67
Collagen subscore	0.02	.76	0.03	.69	0.08	.50	0.36	.12	0.00	.99
Vessel subscore	0.12	.40	0.17	.31	0.11	.41	0.01	.79	0.18	.30
Cell density	0.00	.88	0.01	.79	0.15	.34	0.11	.43	0.13	.36
Vessel density	0.01	.85	0.14	.36	0.02	.75	0.18	.29	0.13	.38
12 months (n = 8)										
LMI	0.06	.54	0.09	.47	0.04	.63	0.12	.39	0.07	.54
Cell subscore	0.19	.28	0.17	.32	0.69 <sup>b</sup>	<.05	0.24	.22	0.11	.43
Collagen subscore	0.08	.49	0.14	.37	0.01	.86	0.30	.16	0.06	.55
Vessel subscore	0.18	.29	0.14	.35	0.10	.44	0.02	.77	0.16	.33
Cell density	0.27	.19	0.43	.08	0.00	.88	0.01	.85	0.30	.16
Vessel density	0.08	.49	0.17	.32	0.10	.45	0.13	.38	0.00	.93
<b>Bioenhanced ACL reconstruction</b>										
6 months (n = 8)										
LMI	0.21	.25	0.23	.23	0.29	.17	0.23	.23	0.07	.52
Cell subscore	0.03	.68	0.05	.61	0.13	.39	0.11	.42	0.01	.78
Collagen subscore	0.28	.18	0.34	.13	0.23	.23	0.24	.21	0.25	.2
Vessel subscore	0.00	.92	0.00	.94	0.14	.36	0.09	.48	0.05	.61
Cell density	0.00	.82	0.02	.77	0.32	.15	0.18	.29	0.06	.56
Vessel density	0.18	.30	0.07	.52	0.44	.07	0.10	.45	0.04	.65
12 months (n = 8)										
LMI	0.70 <sup>b</sup>	<.01	0.78 <sup>b</sup>	<.01	0.08	.50	0.01	.79	0.47	.06
Cell subscore	0.56 <sup>b</sup>	<.05	0.74 <sup>b</sup>	<.01	0.05	.58	0.14	.36	0.32	.15
Collagen subscore	0.71 <sup>b</sup>	<.01	0.87 <sup>b</sup>	<.001	0.04	.66	0.05	.58	0.60 <sup>b</sup>	<.05
Vessel subscore	0.15	.35	0.12	.40	0.13	.39	0.00	.95	0.01	.80
Cell density	0.3	.16	0.25	.20	0.00	.95	0.02	.74	0.30	.16
Vessel density	0.16	.33	0.25	.21	0.14	.36	0.10	.45	0.27	.19

<sup>a</sup>Shown are linear regression coefficients and  $P$  values at 6 and 12 months for each of the 3 groups. LMI, Ligament Maturity Index; ACL, anterior cruciate ligament.

<sup>b</sup>Statistically significant correlation.

comparisons), with a higher cellular subscore consistent with a higher maximum load and linear stiffness. The collagen subscore predicted more than 65% of the variability of the structural properties (maximum load and stiffness) of the healing tissue at 6 months ( $r^2 > 0.66$ ,  $P < .05$  for both variables). However, the LMI vessel subscore was not a significant predictor of the structural properties (maximum load and stiffness) of the repair

tissue at 6 months ( $r^2 > 0.44$ ,  $P > .07$  for both variables). In contrast to the LMI cell subscore, the cell density of the tissue did not correlate significantly with the maximum load or stiffness of the tissue ( $r^2 > 0.05$  for both comparisons). Neither the LMI or its subscores nor densities of cells or vessels were predictive for the material properties (stress, strain, tangent modulus) of the bioenhanced repair group at 6 months (Table 3).

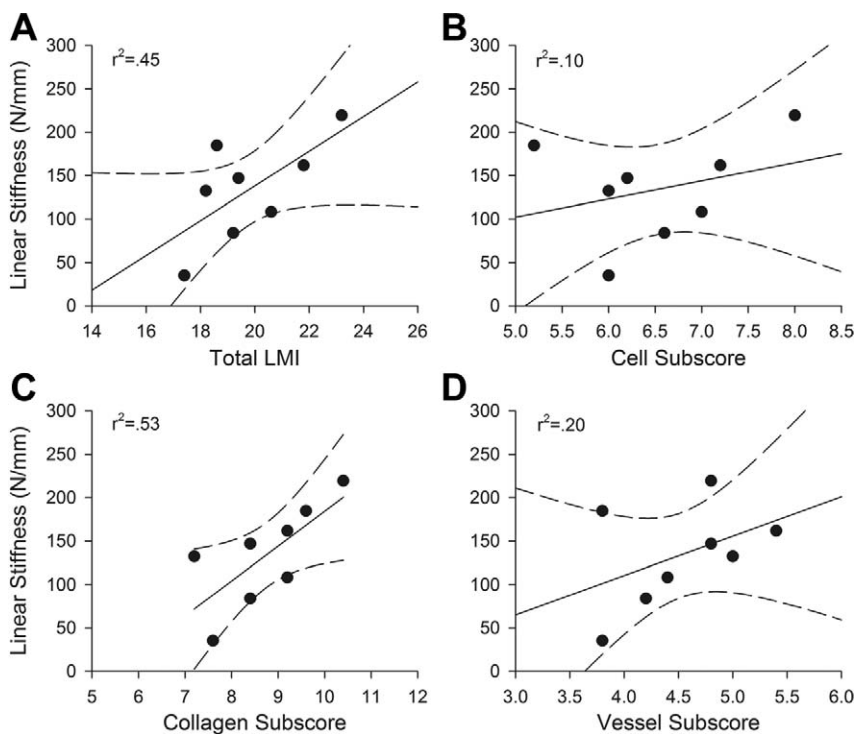


**Figure 4.** Linear stiffness of the bioenhanced ACL repair procedure at 12 months of healing as a function of (A) total LMI, (B) cellular subscore, (C) collagen subscore, and (D) vessel subscore. While higher scores were still seen in the repairs with higher maximum load and stiffness, the correlation was not as strong as at the 6-month time point. ACL, anterior cruciate ligament; LMI, Ligament Maturity Index.

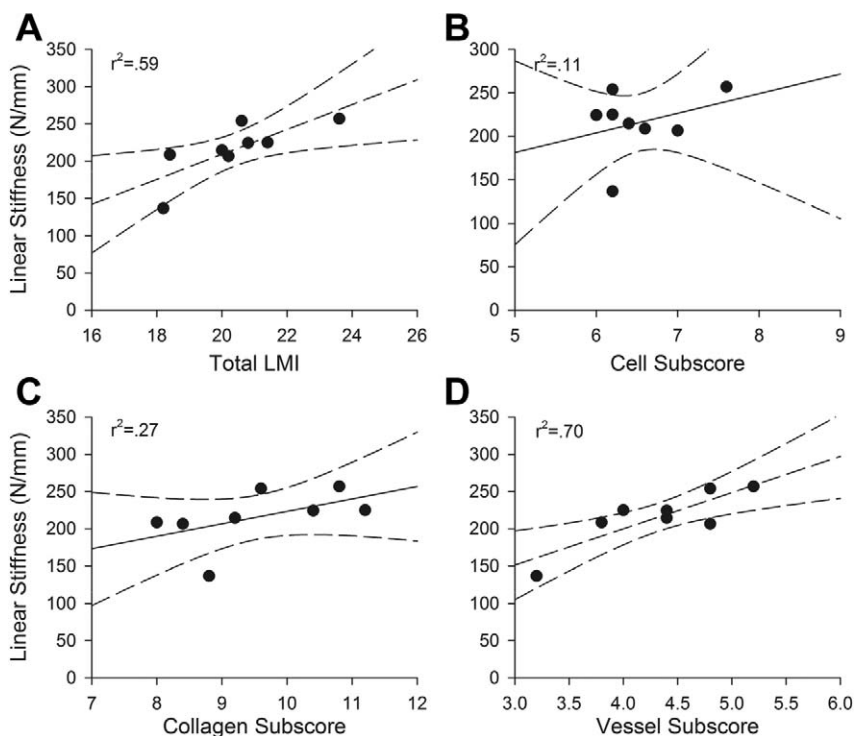


**Figure 5.** Linear stiffness of the ACL reconstruction procedure at 6 months of healing as a function of (A) total LMI, (B) cellular subscore, (C) collagen subscore, and (D) vessel subscore. Dotted lines are 95% confidence intervals for slope. A greater organization of vessels correlated with a higher maximum load for the graft at the 6-month time point. ACL, anterior cruciate ligament; LMI, Ligament Maturity Index.

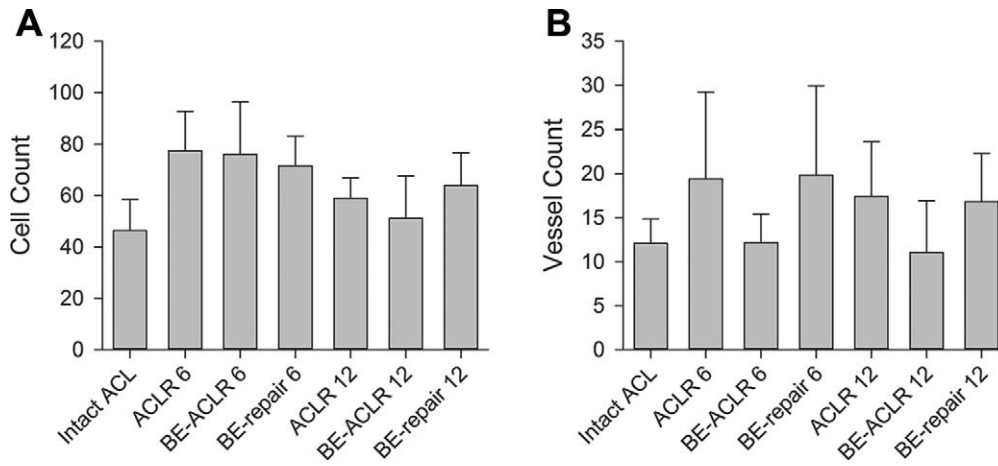


**Figure 6.** Bar graphs of the means of (A) the total cell count per 0.08 mm<sup>2</sup> and (B) the total vessel count per 1.4 mm<sup>2</sup> of the different treatment groups at 6 and 12 months. Error bars show the 95% confidence intervals of the means. ACLR 6, anterior cruciate ligament (ACL) reconstruction after 6 months; ACLR 12, ACL reconstruction after 12 months; BE, bioenhanced.

**TABLE 4**  
Mean Cell Density, Vessel Density, and Cross-Sectional Area for Each Group<sup>a</sup>

Group	Cell Density <sup>b</sup>		Vessel Density <sup>c</sup>		Cross-Sectional Area	
	Mean	SD	Mean	SD	Mean	SD
<b>Bioenhanced repair</b>						
6 months (n = 8)	71.6	11.5	19.8	10.1	76.4	32.2
12 months (n = 8)	64.0	12.7	16.8	5.5	77.3	38.5
<b>ACL reconstruction</b>						
6 months (n = 8)	77.5	15.2	19.4	9.8	113.8	23
12 months (n = 8)	58.9	8.0	17.4	5.9	93.3	49.8
<b>Bioenhanced ACL reconstruction</b>						
6 months (n = 8)	76.1	20.3	12.2	3.2	109.4	48.2
12 months (n = 8)	51.2	16.6	11	5.9	72.7	23.2

<sup>a</sup>ACL, anterior cruciate ligament; SD, standard deviation.

<sup>b</sup>Cells per 0.085 mm<sup>2</sup>.

<sup>c</sup>Vessels per 1.45 mm<sup>2</sup>.

**Bioenhanced Repair: 12 months**

For the structural properties after 12 months of healing, the total advanced LMI (Figure 2) predicted only 51% of the variability of the maximum load ( $r^2 > 0.51, P < .05$ ) (Table 2) and 45% of the linear stiffness of the healing tissue, and this correlation was not statistically significant ( $r^2 > 0.45, P = .08$ ) (Table 2, Figure 4). While higher scores were still seen in the repairs with higher maximum load and linear stiffness, the correlation was not as strong as at the 6-month time point. The cellular subscore was no longer significantly predictive of the structural properties (maximum load and stiffness) of the healing ligament; however, the collagen subscore predicted over 50% of the variability in maximum load and linear stiffness of the repair tissue ( $r^2 > 0.50$  and  $P < .02$  for both variables). The vessel subscore was not predictive of structural properties (maximum load and stiffness) at the 12-month time point ( $r^2 > 0.07, P > .54$  and

$r^2 > 0.2, P > .27$ , respectively). Neither cell density nor vessel density were significantly predictive of the strength of the ACL repair tissue ( $r^2 > 0.25, P > .21$  and  $r^2 > 0.04, P > .64$ , respectively). For material properties, the advanced LMI predicted 75% of the yield stress and 71% of the maximum stress ( $P < .01$  for both) (Table 3). This was true for the cell subscores as well as the collagen subscores (Table 3).

**ACL Reconstruction: 6 months**

For the structural properties, the advanced LMI (Figure 2) was predictive of yield load, maximum load, and linear stiffness of the grafts at 6 months ( $r^2 > 0.59$  and  $P < .05$  for all correlations) (Table 2, Figure 5). The vessel subscore also correlated significantly with the structural properties (yield load, maximum load, and linear stiffness) of the grafts at 6 months (Table 2). However, while the collagen subscore correlated with structural properties (yield load, maximum load), no significant correlation was found for linear stiffness (Table 2, Figure 5). The cellular subscore was not predictive of any of the mechanical outcomes. Neither the advanced LMI nor its subscores were predictive of the material properties of the ACL grafts at 6 months (Table 3).

**ACL Reconstruction: 12 months**

After 12 months of healing, only the cell density of the graft was significantly predictive of the structural properties (yield and maximum loads) of the ACL graft ( $r^2 > 0.50, P < .008$ ) (Table 2). A higher cell number within the graft was predictive of a higher maximum load of the graft.

**Bioenhanced ACL Reconstruction: 6 and 12 months**

There were no significant histological predictors of graft structural properties (yield load, maximum load, or linear stiffness) for the group treated with bioenhanced reconstruction after either 6 or 12 months of healing in vivo (Table 2). In



TABLE 5  
Ligament Maturity Index (LMI) Scores and Subscores<sup>a</sup>

Group	LMI Subscore							
	LMI		Cellularity		Collagen		Vascularity	
	Mean	SD	Mean	SD	Mean	SD	Mean	SD
Bioenhanced repair								
6 months (n = 8)	18.9	3.0	6.4	0.6	8.4	2.0	4.2	0.7
12 months (n = 8)	19.8	1.9	6.5	0.9	8.8	1.1	4.5	0.6
ACL reconstruction								
6 months (n = 8)	20.4	1.7	6.5	0.5	9.6	1.2	4.3	0.6
12 months (n = 8)	20.7	0.8	7.1	0.4	9.7	0.7	4.9	0.7
Bioenhanced ACL reconstruction								
6 months (n = 8)	21.1	2.2	6.8	0.7	9.5	1.0	4.8	0.8
12 months (n = 8)	21.7	1.9	7.5	0.6	9.9	1.0	5.4	0.7

<sup>a</sup>ACL, anterior cruciate ligament; SD, standard deviation.

contrast, for the material properties, the yield stress as well as maximum stress for the bioenhanced ACL reconstruction group at 12 months were significantly predicted by the advanced LMI ( $r^2 > 0.7$ ,  $P < .01$  for both) (Table 3), the cellular subscore ( $r^2 > 0.56$ ,  $P < .01$  for both) (Table 3), and the collagen subscore ( $r^2 > 0.71$ ,  $P < .01$  for both) (Table 3). More than 60% of the tangent modulus was predicted by the collagen subscore at the same time point ( $r^2 > 0.6$ ,  $P < .05$ ) (Table 3).

#### Anteroposterior Knee Laxity and Location of Failure

The anteroposterior knee laxity data have been previously reported.<sup>16</sup> There was no significant correlation between anteroposterior laxity and any of the histological parameters. For the biomechanical testing, the specimens failed in the midsubstance of the repaired ligament or graft.

#### Mean Comparisons Across Groups

There were no significant differences found between treatment groups in terms of the advanced LMI score or subscores or the cell and vessel density at either 6 or 12 months (Figures 2 and 6, Tables 4 and 5). There was a significant decrease in the cell density in the bioenhanced reconstruction group between 6 and 12 months (76.1 vs 51.2,  $P < .05$ ) (Figure 6, Table 4). Cell density decreased as well in the bioenhanced repair and the reconstruction group from 6 to 12 months but not significantly ( $P = 1.0$  and  $P = .26$ , respectively) (Table 4).

#### DISCUSSION

In this study, we found that the treatment method used to treat the ACL injury was not predictive of the histological appearance of the tissue at 6 and 12 months after healing. Ligaments treated with bioenhanced ACL repair, ACL reconstruction, and bioenhanced ACL reconstruction all had similar histological appearances. Generally speaking, enhanced primary ACL repair achieved the same properties as an ACL reconstruction—the current gold standard

of ACL tear treatment. This finding suggests potential promise for this new method of treatment and its eventual use in clinical care. However, within the bioenhanced repair group and reconstruction group, the degree of cellular, collagen, and vessel organization correlated with the mechanical properties of the new ACL tissue. Interestingly, the factors that were most predictive of the biomechanical performance were different between these treatment groups.

For example, at 6 months after surgery, the maximum load and linear stiffness values of the ligaments treated with bioenhanced repair were higher in those ligaments with a more organized cellular pattern, as shown by a high correlation of cellularity and yield load, while the same biomechanical parameters of the ligaments treated with an ACL reconstruction were not dependent on cellular organization but on the degree of organization of the collagen. At 12 months of healing, the ligaments treated with bioenhanced repair were then dependent on collagen organization rather than cellular density or organization, while the ACL reconstruction graft function only correlated with the total cellular number in the grafts, with those grafts with higher cell number in the graft having a higher maximum load, and was not significantly correlated with the degree of organization of those cells.

In general, the correlations between the histological scores and mechanical properties were higher for the bioenhanced repairs ( $r^2$  values between 0.28 and 0.79) than the ACL reconstructions ( $r^2$  values between 0.01 and 0.89). This may reflect a higher dependency on biological processes for developing strength in the repaired ligament than for a reconstruction graft, emphasizing the differences between ligament healing and graft “ligamentization.” For repairs, the provisional scaffold starts out as a structure free of fibroblasts and collagen. The fibroblasts from surrounding tissues then invade the scaffold and begin to produce new collagen in a relatively random fashion.<sup>1,19</sup> It is this newly produced, disorganized collagen that confers strength of the healing tissue, and over time, that collagen within the scar becomes more organized.<sup>10,15</sup> In our study, it appears that in the first 6 months, the organization of

that collagen is likely less important to overall scar strength than the organization of the cells producing it. It is possible that the higher degree of cellular organization may lead to improved collagen alignment in the newly deposited collagen. Another possibility is that in some ligaments, the early collagen deposition has an improved longitudinal alignment, which in turn leads to improved cell alignment within the deposited collagen. Establishing either of these hypotheses as the true mechanism is beyond the scope of this study. In contrast, an ACL graft starts with well-aligned collagen in densely packed bundles. Cellular invasion of the graft is slower than into a provisional scaffold, often taking weeks rather than days,<sup>2,3</sup> and the contribution of newly produced collagen to graft strength is likely less important than retention of the overall initial collagen organization or the initial fixation strength of the implanted graft. In addition, for the healing tissue of the bioenhanced ACL repairs, which is often disorganized in the early healing phases, the cellular organization may be required prior to the deposition of more orderly collagen, and thus, the cellular subscore may simply be a marker for upcoming collagen organization.

It is unclear why the vessel subscores did not play more of a role in the correlation with mechanical properties of the tissues. The scores were similar among groups. The lack of significant correlation may be because of the fact that the subscore of the LMI is not measuring the critical elements of revascularization (as it only addresses qualitative organization, density, and type), or that the technique of analyzing sagittal sections does not allow us to fully appreciate the 3-dimensional morphometry of the vascular structures of the ligament sufficiently. Using microsphere assessment of blood flow to rabbit medial collateral ligaments after wounding, Bray et al<sup>5</sup> found an increase in blood flow between 3 and 6 weeks, which was no longer statistically significantly increased by 17 weeks. Quantitative histological assessment combined with ink-gelatin perfusion in the same model reported the vessel density returning to normal values between 17 and 40 weeks after injury.<sup>5</sup> Using vascular injection techniques in a goat model, revascularization of the grafts has been reported to be complete by 12 weeks.<sup>6</sup> Thus, our time points of 26 and 52 weeks may be past the period where significant vascular changes are still occurring in the healing ACL, and even our advanced vessel subscore may thus be less useful in the later stages of ligament or graft healing.

It was also of interest that the mechanical properties of the bioenhanced ACL reconstructions did not correlate with any of the histological measures. This group of grafts was the most mature histologically, with the highest mean scores in the cellular, collagen, and vessel subscores, although the differences between groups were not found to be statistically significant, likely in part because of the large number of comparisons and the biological variability in each group and the sensitivity of the caliper measurement technique used to measure the length and cross section of the healing ligament. That being said, it may be that the bioenhanced ACL reconstructed grafts may have matured earlier and thus reached the "ceiling" for this index prior to the 6-month time point, much the way the ACL reconstructed grafts did at the 12-month time point.

Another interesting finding was the correlation of yield and maximum stress with the cellular and collagen subscores as well as the advanced LMI in the bioenhanced repair and bioenhanced ACL reconstruction group at 12 months. While cellular subscore, collagen subscore, and LMI seem to predict these material properties well at 12 months, they seem to predict structural properties better at 6 months in these 2 groups. The material properties are independent of the cross-sectional area of the ACL; the structural properties are not. Hence, for the bioenhanced groups at 6 months, the difference in the organizational state of the fibroblasts that initially invaded the scaffold as well as their newly produced collagen seems to be more important for the mechanical strength of the ACL than the cross-sectional area. At 12 months, the maturation and organization of the fibroblasts and collagen may be mostly completed in all of the ligaments, thus making the structural properties more dependent on the thickness of the healed ligament.

There are several limitations to this study. First, the study was conducted in an animal model rather than in human patients. Although the porcine model is similar to the human knee in terms of biomechanical function and ACL dependence,<sup>4</sup> the porcine knee does not gain full extension and the porcine model is a quadruped rather than biped. In addition, the freeze-thaw cycle that the knee specimens went through potentially affected histological findings of ligament tissue. To minimize this process having a differential effect in groups, all knees were frozen and thawed with an identical protocol to minimize variability. Also, the histological analyses were performed after biomechanical testing had been conducted. During tensile testing, the ligament will have reversible flattening of the crimp followed by a point of inelastic deformation.<sup>11</sup> In this experiment, the use of a servohydraulic load frame allowed for a very slow and controlled pull of the ligament, which enabled us to stop the test just after the drop in load occurred but prior to the complete disruption of the ligamentous tissue to minimize irreversible changes during the mechanical testing. In addition, the majority of the specimens failed in the midsubstance, and a defect was visible at the failure site. This local region was not included in the histological analysis because of concerns that it may have been damaged during the failure process. The 5 sites of analysis for each ligament had no consistent or significant pattern of difference among groups, suggesting a relative uniformity of the histological findings throughout the ligament. In addition, prior studies have demonstrated that by 3 months after injury, the histological appearance of the healing ligament and reconstruction grafts are relatively uniform.<sup>12</sup>

In addition, one would not anticipate the cellular or vascular distribution throughout the ligament to change significantly with tensile testing. While we avoided analysis of regions that were at the site of ligament rupture, it is possible that the crimp length portion of the collagen subscores may have been affected by this prior testing. The bundle width and orientation were less likely to be altered with the longitudinal tensile testing of this relatively mature tissue. Lastly, as all specimens underwent identical testing, it was thought any changes in the collagen

subscores would be relatively uniform within each group and thus not disturb the regression analyses. With these limitations in mind, particularly that of the crimp length variable, we elected to still proceed with the histological analysis after testing, as this was the only way to directly correlate mechanical function with histological findings in each animal.

## CONCLUSION

The data show that cellular and collagen subscores of the advanced LMI correlate with structural properties of the healing ligament and ACL reconstruction grafts after 6 months of healing. At 12 months, the collagen subscore correlated with structural properties for the repaired ligaments only, whereas advanced LMI and cellular and collagen subscore were predictive for the material properties. The qualitative histological measure used here may thus be useful in understanding the requisite biological processes of wound healing and the development of wound strength in the first 6 months after injury; however, after 12 months of healing, only the organization of the collagen in the wound appears to correlate with wound strength, and this index may be less useful.

## ACKNOWLEDGMENT

The authors thank Dr Patrick Vavken, Elise Magarian, and Carla Haslauer for their assistance in surgery and tissue collection, and the ARCH staff, Dr Arthur Nedder, Kathryn Mullen, Dana Bolgen, and Courtney White, for their assistance and care in handling the animals. The authors also thank David Paller, Alison Bierciewicz, and Sarath Korupolu for the conduction of the biomechanical testing, as well as David Zurakowski for the statistical analysis.

## REFERENCES

- Amiel D, Frank CB, Harwood FL, Akeson WH, Kleiner JB. Collagen alteration in medial collateral ligament healing in a rabbit model. *Connect Tissue Res.* 1987;16:357-366.
- Amiel D, Kleiner JB, Akeson WH. The natural history of the anterior cruciate ligament autograft of patellar tendon origin. *Am J Sports Med.* 1986;14:449-462.
- Amiel D, Kleiner JB, Roux RD, Harwood FL, Akeson WH. The phenomenon of "ligamentization": anterior cruciate ligament reconstruction with autogenous patellar tendon. *J Orthop Res.* 1986;4:162-172.
- Boguszewski DV, Shearn JT, Wagner CT, Butler DL. Investigating the effects of anterior tibial translation on anterior knee force in the porcine model: is the porcine knee ACL dependent? *J Orthop Res.* 2011;29:641-646.
- Bray RC, Rangayyan RM, Frank CB. Normal and healing ligament vascularity: a quantitative histological assessment in the adult rabbit medial collateral ligament. *J Anat.* 1996;188(pt 1):87-95.
- Drez DJ Jr, DeLee J, Holden JP, Arnoczky SP, Noyes FR, Roberts TS. Anterior cruciate ligament reconstruction using bone-patellar tendon-bone allografts. A biological and biomechanical evaluation in goats. *Am J Sports Med.* 1991;19:256-263.
- Fisher MB, Liang R, Jung HJ, et al. Potential of healing a transected anterior cruciate ligament with genetically modified extracellular matrix bioscaffolds in a goat model. *Knee Surg Sports Traumatol Arthrosc.* 2012;20:1357-1365.
- Fleming BC, Carey JL, Spindler KP, Murray MM. Can suture repair of ACL transection restore normal anteroposterior laxity of the knee? An ex vivo study. *J Orthop Res.* 2008;26:1500-1505.
- Fleming BC, Spindler KP, Palmer MP, Magarian EM, Murray MM. Collagen-platelet composites improve the biomechanical properties of healing anterior cruciate ligament grafts in a porcine model. *Am J Sports Med.* 2009;37:1554-1563.
- Frank CB. Ligament structure, physiology and function. *J Musculoskelet Neuronal Interact.* 2004;4:199-201.
- Goulam Houssen Y, Gusachenko I, Schanne-Klein MC, Allain JM. Monitoring micrometer-scale collagen organization in rat-tail tendon upon mechanical strain using second harmonic microscopy. *J Biomech.* 2011;44:2047-2052.
- Joshi S, Mastrangelo A, Magarian E, Fleming BC, Murray MM. Collagen-platelet composite enhances biomechanical and histologic healing of the porcine anterior cruciate ligament. *Am J Sports Med.* 2009;37:2401-2410.
- Katsuragi R, Yasuda K, Tsujino J, Keira M, Kaneda K. The effect of nonphysiologically high initial tension on the mechanical properties of in situ frozen anterior cruciate ligament in a canine model. *Am J Sports Med.* 2000;28:47-56.
- Ma J, Smetana MJ, Kostrominova TY, Wojtyls EM, Larkin LM, Arruda EM. Three-dimensional engineered bone-ligament-bone constructs for anterior cruciate ligament replacement. *Tissue Eng Part A.* 2012; 18:103-116.
- Mastrangelo AN, Haus BM, Vavken P, Palmer MP, Machan JT, Murray MM. Immature animals have higher cellular density in the healing anterior cruciate ligament than adolescent or adult animals. *J Orthop Res.* 2010;28:1100-1106.
- Murray MM, Fleming BC. Use of a bioactive scaffold to stimulate anterior cruciate ligament healing also minimizes post-traumatic osteoarthritis after surgery. *Am J Sports Med.* 2013;41:1762-1770.
- Murray MM, Magarian EM, Harrison SL, Mastrangelo AN, Zurakowski D, Fleming BC. The effect of skeletal maturity on functional healing of the anterior cruciate ligament. *J Bone Joint Surg Am.* 2010;92:2039-2049.
- Murray MM, Spindler KP, Ballard P, Welch TP, Zurakowski D, Nannery LB. Enhanced histologic repair in a central wound in the anterior cruciate ligament with a collagen-platelet-rich plasma scaffold. *J Orthop Res.* 2007;25:1007-1017.
- Shrive N, Chimich D, Marchuk L, Wilson J, Brant R, Frank C. Soft-tissue "flaws" are associated with the material properties of the healing rabbit medial collateral ligament. *J Orthop Res.* 1995;13: 923-929.
- Vavken P, Fleming BC, Mastrangelo AN, Machan JT, Murray MM. Biomechanical outcomes after bioenhanced anterior cruciate ligament repair and anterior cruciate ligament reconstruction are equal in a porcine model. *Arthroscopy.* 2012;28:672-680.